Supplemental Methods

Stimulated Emission Depletion (STED) confocal microscopy. ATTO-647N labeled Phalloidin (30 nM in 1% DMSO, Atto-tec, Siegen, Germany) was applied to plated DRGs for 10 min prior to being fixed, washed and mounted following specific guidelines for sample preparation (48). High-resolution images shown in SFig. 3 were obtained using a Leica TCS SP5 STED confocal system (Leica Microsystems, Wetzlar, Germany) equipped with an oil immersion objective (HCX PL APO CS 100x/1.40NA STED). A 635nm pulsed diode laser (PicoQuant, Germany) was used for excitation. The pulses for STED depletion were delivered using a tunable ultrafast Ti:Sapphire laser (Mai Tai® Broadband, Spectra-Physics, CA) emitting at a wavelength of 750 nm. Red fluorescence emitted from an ATTO 647N–labeled Phalloidin was collected through a Semrock BrightLine® 685/40-25 nm band pass filter (FF01-685/40-25, Semrock, Rochester, NY) in front of an avalanche photodiode (APD, PerkinElmer, Waltham, MA).

Suppemental Figure Legends

SFig. 1 *Ca^{2+} channel density, type and constitutive δOR-VDCC coupling are not regulated by β-arr1- related to Figure 1.* A.i. A successive voltage step protocol was used to examine Ca^{2+} current density. Examples of these recordings from early postnatal β-arr1-/- and +/+ neurons are shown above the line graph, which in depicting the current-voltage relationship (ii), indicates no effect of β-arrestin 1 on Ca^{2+} current density. B. The relative contribution of the N, P/Q and L-Ca^{2+} channels to the Ca^{2+} current was also examined by inhibiting each channel. i. After obtaining a stable basal Ca^{2+} current (1), ω-Conotoxin GVIA (10μM, 1% cytochrome C) was used to inhibit the N-type channel (2). ii. A similar protocol was used to inhibit the P/Q-type channels before (1) and during (2) the application of Agatoxin IVA (100nM). iii. The

contribution of the L-type channels was assessed by Nifedipine (3, 10μM, 0.1% DMSO) after a stable baseline was obtained (1) and the N-type was fully inhibited by ω-Conotoxin GVIA (2). The resulting inhibition, expressed as a percent of the total Ca^{2+} current, showed no effect of genotype on the relative contribution of the N (i) , P/Q (ii) or L-type (iii) Ca^{2+} currents. C. Constitutive inhibition of the VDCCs was examined by a 2-step protocol. Examples of this protocol, which uses a high voltage pre-pulse to dissociate constitutively coupled $G_{\beta\gamma}$ subunits from Ca^{2+} channels are shown (i), 1 indicates the current measured without a pre-pulse (P1) and 2 (P2) that recorded after the pre-pulse is applied. The P2/P1 ratio, reflecting constitutive Ca^{2+} channel coupling, was increased in the large, but not small DRG neurons. This ratio was further enhanced in β-arr1-/- neurons. ii. However, ICI 174.864, a δOR inverse agonist, could not reverse the enhanced effect in the β-arr1-/- neurons suggesting that although there is evidence of enhanced constitutive coupling of $G_{\beta\gamma}$ subunits with VDCCs, this is not mediated by δORs. All pooled data are shown as mean±SEM.

SFig. 2 *Flow Cytometry assessment of δOR antibody specificity- related to Figure 2.* DRG neurons from δOR +/+ and -/- early postnatal mice were cultured for 48h, re-suspended and labeled with an antibody to the N-terminus of the human δOR sequence (MBL) followed by an APC-conjugated secondary and analyzed by flow cytometry. Unlabeled δOR+/+ neurons that had not been incubated with either antibody were included. Using the same template as shown in Fig. 2Ci to select medium-large sized neurons, scatterplots of the fluorescence intensity of the unlabeled and labeled δOR-/- and +/+ neurons are shown (1 dot=1 cell). These plots show no

difference in labeling between the unlabeled and δOR -/- samples whereas the δOR +/+ sample shows a greater percentage of APC or δOR-positive cells.

SFig. 3 *SNC80 internalizes cerulean-tagged δORs in both β-arr1+/+ and -/- DRG neurons- related to Figure 2.* After 1h of SNC80 (1μM), virally expressed cerulean-tagged δORs, demonstrate equivalent internalization, when imaged by epifluorescence, in cultured β-arr1+/+ and -/- DRG neurons. The cell bodies and processes from untreated DRGs are shown in a and b respectively whereas c and d show the cell bodies and processes from SNC80-treated DRG neurons. The top and bottom rows are of β-arr1+/+ and -/- neurons. Scale-bar=10μm. Images were acquired on a Nikon TE2000 using a 60x objective and imaged by a Retiga1300 CCD and Iplab v4 (Qimaging, Ontario, CA).

SFig. 4 *Basal F-actin incorporation is not altered in β-arr1-/- neurons- related to Figure 4.* β-arr1+/+ and -/- neurons were incubated with Phalloidin-Atto647N for 10 min at 37°C, fixed and imaged by STED microscopy. There was no apparent effect of genotype on Phalloidin incorporation in the cell bodies and processes of β-arr1+/+ (a and b respectively) and -/- (c and d respectively) neurons. Scale-bar=2μm.

SFig. 5 *The behavioral effects of a delta agonist are similarly enhanced in β-arr1-/- and +/+ mice in the C57BL/6 background- related to Figure 5.* A. Fentanyl produced a hyperlocomotor response in β-arr1+/+ ($p<0.05$, $F_{2,21}=5.03$ locomotion x treatment) and in β-arr1-/- mice ($p<0.01$, $F_{2,23}=7.80$ locomotion x treatment), which was unaffected by pretreatment with the ROCK inhibitor, Y27632. Furthermore, no differences were observed in fentanyl-induced locomotion

between the two genotypes ($p=0.92$, $F_{1,10}=0.01$), *$p<0.05$ vs. other treatment groups. B. SNC80 (1mg/kg s.c.) produced a hyperlocomotor response in β-arr1+/+ ($p<0.05$, $F_{1,17}=6.31$ vs. vehicle), β-arr1-/- ($p<0.001$, $F_{1,19}=78.13$ vs. vehicle), β-arr2+/+ ($p<0.01$, $F_{1,18}=9.62$ vs. vehicle), as well as, β-arr2-/- ($p<0.05$, $F_{1,17}=7.85$ vs. vehicle) in the C57Bl/6 background. However, this effect was enhanced in β-arr1-/- mice as compared to the other three groups ($p<0.05$, $F_{3,33}=4.255$ locomotion x genotype) **$p<0.01$, *$p<0.05$ vs. other groups receiving the same treatment. C. The Von-Frey test for mechanical allodynia was used to measure sensitivity to mechanical pain on the plantar surface of the right paw after vehicle or SNC80 (5 mg/kg s.c.). While both groups showed similar basal responses ($p=0.98$), and SNC80 had no effect in β-arr1+/+ mice, β-arr1-/- mice responded less than +/+ mice 20 and 40 min after the SNC80 injection ($p<0.001$, $F_{1,27}=53.41$ vs. β-arr1+/+). All data are shown as mean±SEM.

SFig. 1

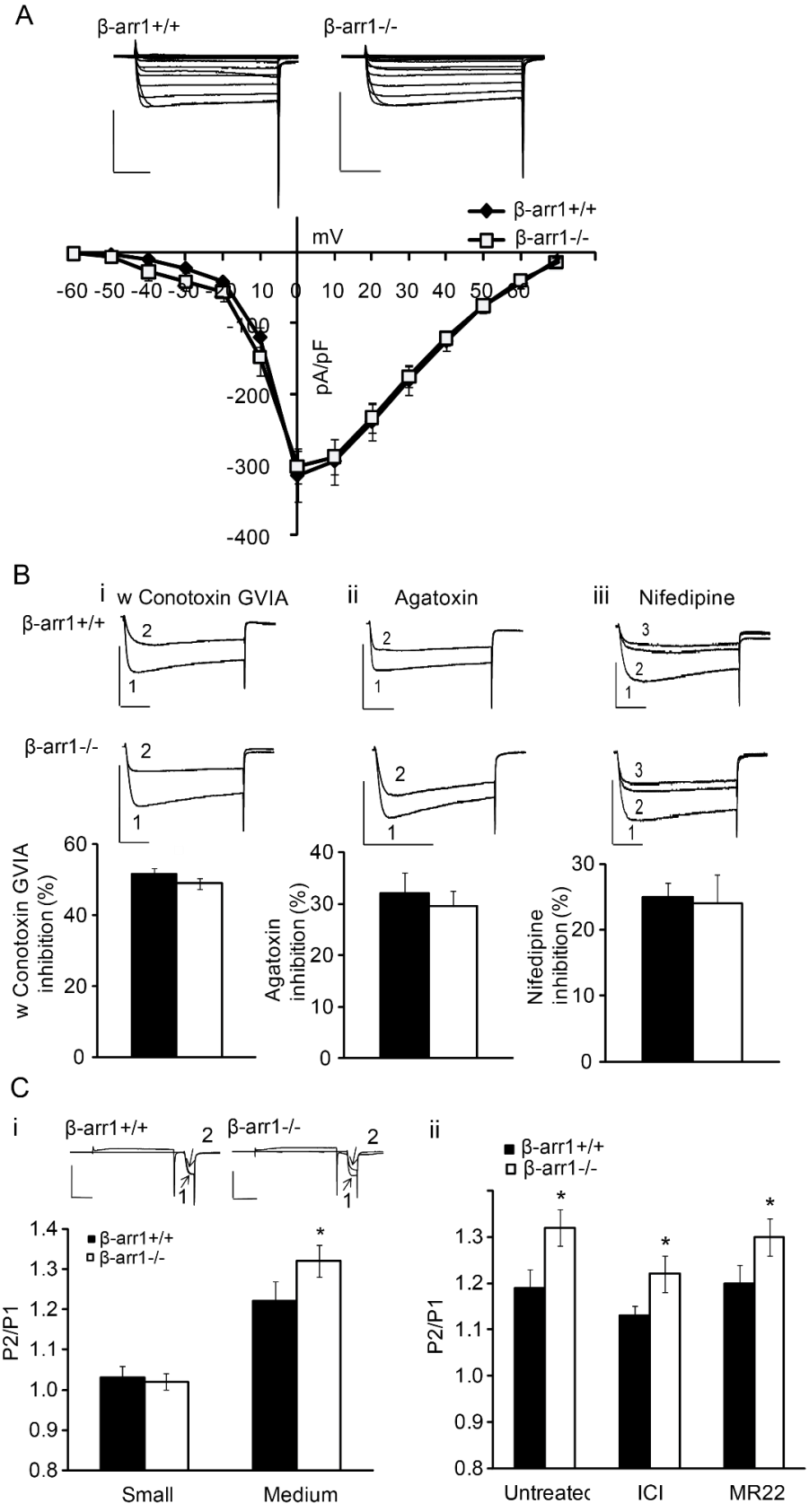
A
β-arr1+/+
β-arr1-/-
mV
β-arr1+/+
β-arr1-/-
-60 -50 -40 -30 -20 10 0 10 20 30 40 50 60
-100
-200
-300
-400
pA/pF
B
i w Conotoxin GVIA
ii Agatoxin
iii Nifedipine
β-arr1+/+
β-arr1-/-
1
2
3
w Conotoxin GVIA inhibition (%)
Agatoxin inhibition (%)
Nifedipine inhibition (%)
C
i
β-arr1+/+
β-arr1-/-
P2/P1
Small
Medium
ii
β-arr1+/+
β-arr1-/-
P2/P1
Untreated
ICI
MR22

SFig. 2

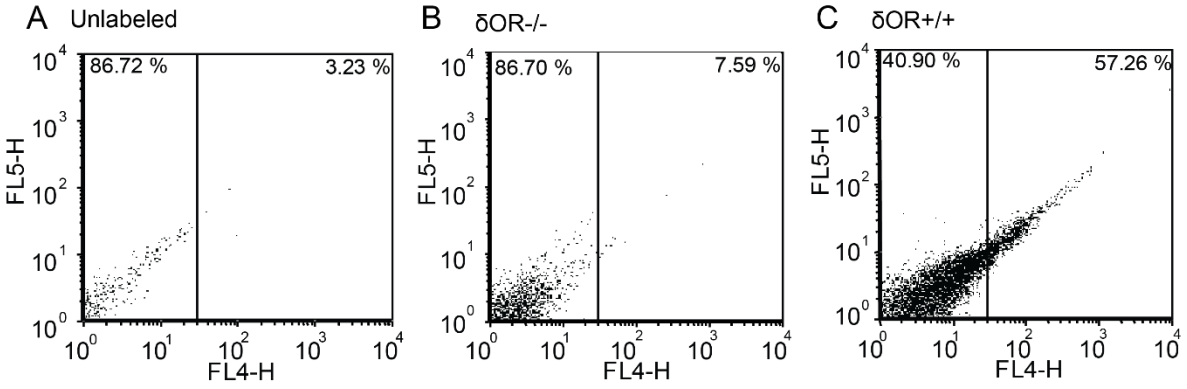

SFig 3

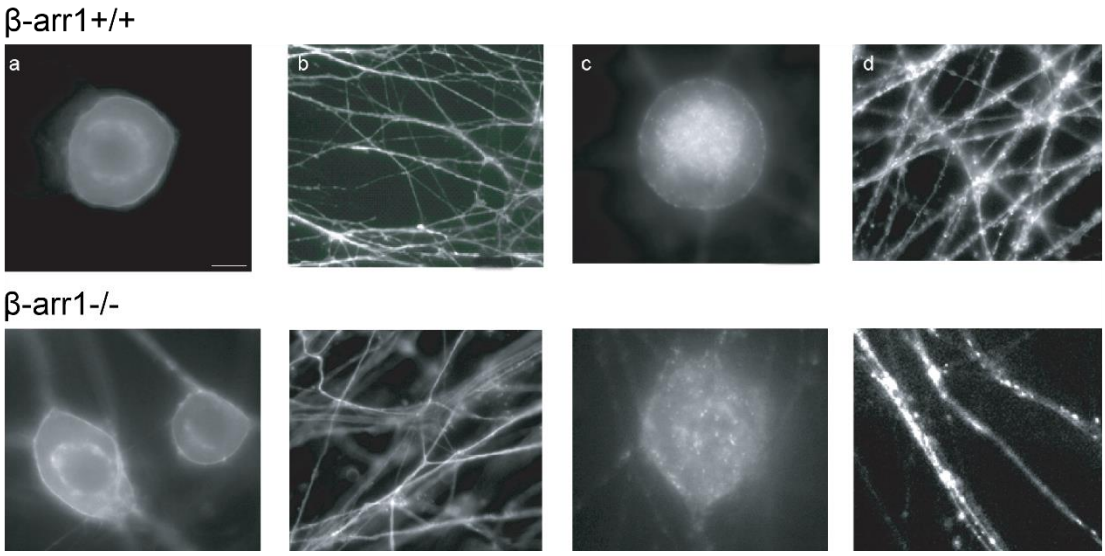

SFig. 4

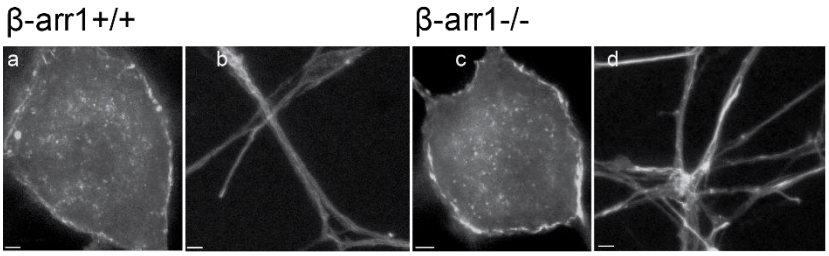

SFig. 5

A

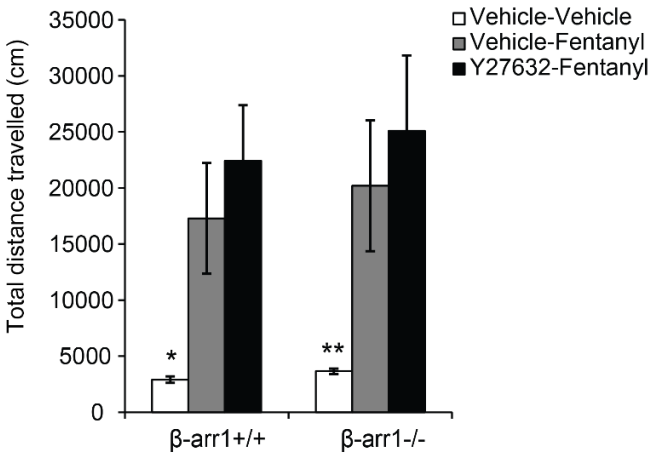
Vehicle-Vehicle
Vehicle-Fentanyl
Y27632-Fentanyl
Total distance travelled (cm)
35000
30000
25000
20000
15000
10000
5000
0
*
**
β-arr1+/+
β-arr1-/-

B

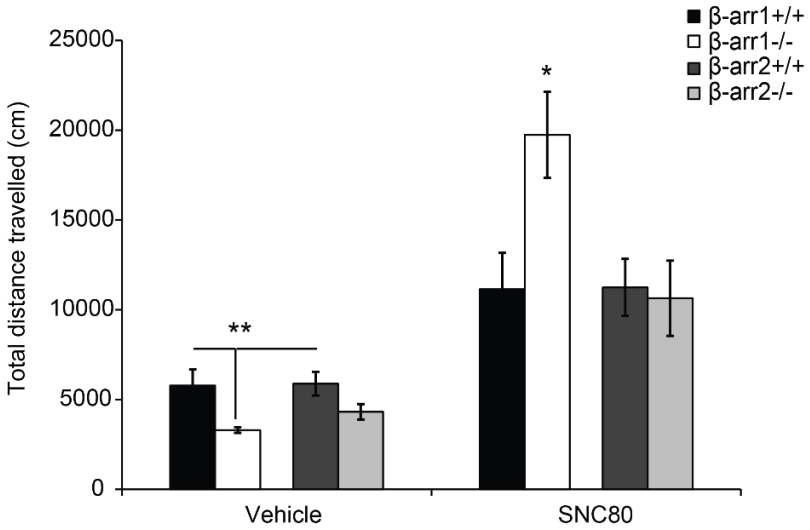
β-arr1+/+
β-arr1-/-
β-arr2+/+
β-arr2-/-
Total distance travelled (cm)
25000
20000
15000
10000
5000
0
**
*
Vehicle
SNC80

C

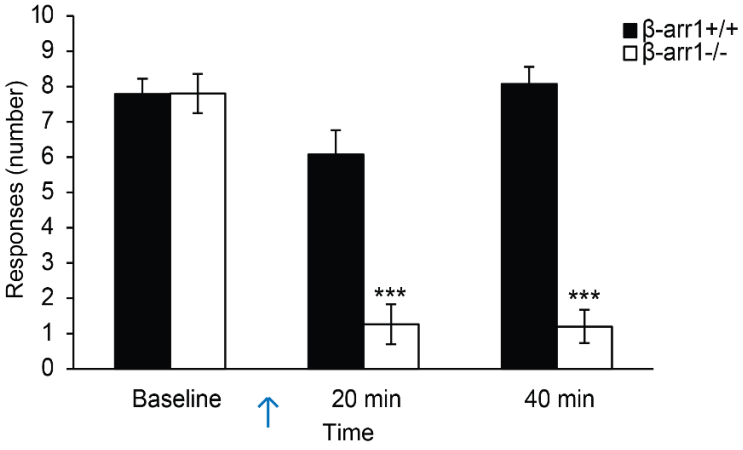
β-arr1+/+
β-arr1-/-
Responses (number)
10
9
8
7
6
5
4
3
2
1
0
***
***
Baseline
20 min
40 min
Time